molecular pharmaceutics

articles

Cationic Shell-Cross-Linked Knedel-like (cSCK) Nanoparticles for Highly Efficient PNA Delivery

Huafeng Fang,[†,‡] Ke Zhang,[†,‡,§] Gang Shen,[†] Karen L. Wooley,*[,†,§] and John-Stephen A. Taylor*[,†]

Department of Chemistry, Washington University, One Brookings Drive, St. Louis, Missouri 63130, and Department of Radiology, Washington University School of Medicine, 510 South Kingshighway Boulevard, St. Louis, Missouri 63110

Received October 13, 2008; Revised Manuscript Received January 15, 2009; Accepted February 20, 2009

Abstract: Peptide nucleic acids have a number of features that make them an ideal platform for the development of *in vitro* biological probes and tools. Unfortunately, their inability to pass through membranes has limited their *in vivo* application as diagnostic and therapeutic agents. Herein, we describe the development of cationic shell-cross-linked knedel-like (cSCK) nanoparticles as highly efficient vehicles for the delivery of PNAs into cells, either through electrostatic complexation with a PNA·ODN hybrid, or through a bioreductively cleavable disulfide linkage to a PNA. These delivery systems are better than the standard Lipofectamine/ODN-mediated method and much better than the Arg_9-mediated method for PNA delivery in HeLa cells, showing lower toxicity and higher bioactivity. The cSCKs were also found to facilitate both endocytosis and endosomal release of the PNAs, while themselves remaining trapped in the endosomes.

Keywords: PNA; nanoparticle; cationic; shell-cross-linked; transfection; bioreductively cleavable linker; endosome; splice correction; cell penetrating; endosome disruption

Peptide nucleic acid (PNA) has a number of properties that make it an ideal platform for the development of antisense- and antigene-based diagnostic and therapeutic agents.[1−5] PNA is highly resistant to degradation by biological systems, hybridizes to a cDNA or RNA strand with higher affinity than DNA, is able to invade regions of secondary structure, and does not activate RNase H, which would otherwise degrade a target mRNA sequence. It is also readily amenable to synthesis by solid phase automated peptide synthesis, which allows the facile preparation of PNA-peptide hybrids and the incorporation of a wide variety of amino acid analogues and auxiliary agents. Despite these advantages, its poor membrane permeability has limited its widespread application for *in vitro* and *in vivo* purposes. There have been numerous attempts to improve PNA's ability to enter cells, which have largely focused on the use

* Authors to whom correspondence should be addressed. K.L.W.: Department of Chemistry, Washington University, One Brookings Dr., St. Louis, MO 63130-4899; phone, 314-935-7136; fax, 314-935-9844; e-mail, klwooley@wustl.edu. J.-S.A.T.: Department of Chemistry, Washington University, One Brookings Dr., St. Louis, MO 63130-4899; phone, 314-935-6721; fax, 314-935-4481; e-mail, taylor@wustl.edu.

† Department of Chemistry, Washington University.

‡ These authors contributed equally to this work.

§ Department of Radiology, Washington University School of Medicine.

(1) Nielsen, P. E. PNA Technology. *Mol. Biotechnol.* **2004**, *26* (3), 233–48.

(2) Zhilina, Z. V.; Ziemba, A. J.; Ebbinghaus, S. W. Peptide nucleic acid conjugates: synthesis, properties and applications. *Curr. Top. Med. Chem.* **2005**, *5* (12), 1119–31.

(3) Porcheddu, A.; Giacomelli, G. Peptide nucleic acids (PNAs), a chemical overview. *Curr. Med. Chem.* **2005**, *12* (22), 2561–99.

(4) Lundin, K. E.; Good, L.; Stromberg, R.; Graslund, A.; Smith, C. I. Biological activity and biotechnological aspects of peptide nucleic acid. *Adv. Genet.* **2006**, *56*, 1–51.

(5) Hu, J.; Corey, D. R. Inhibiting Gene Expression with Peptide Nucleic Acid (PNA)-Peptide Conjugates That Target Chromosomal DNA. *Biochemistry* **2007**, *46* (25), 7581–9.

(6) Braasch, D. A.; Corey, D. R. Synthesis, analysis, purification, and intracellular delivery of peptide nucleic acids. *Methods* **2001**, *23* (2), 97–107.

(7) Braasch, D. A.; Corey, D. R. Lipid-mediated introduction of peptide nucleic acids into cells. *Methods Mol. Biol.* **2002**, *208*, 211–23.

10.1021/mp800199w CCC: $40.75
Published on Web 02/20/2009

of cationic lipids in conjunction with a complementary ODN,[6,7] and covalently attached cell penetrating peptides and lipids.[5,8−10]

Since their inception, nanoparticles have been investigated as carriers and intracellular delivery agents for antisense oligonucleotides, siRNA, and DNA with varying degrees of success.[11−15] We have previously shown that shell-cross-linked knedel-like nanoparticles (SCKs) can be made to efficiently enter cells when derivatized with a cell penetrating peptide.[14,16,17] SCKs are a member of a large family of cross-linked block copolymer micelles that have shown great potential and versatility for biotechnology and medicine due to the ease by which the shape, composition, functionality, and properties can be tailored for a particular purpose.[18] Herein, we report the use of a newly developed class of SCK nanoparticles, called cationic SCKs, or cSCKs, to deliver PNAs into cells without the need to attach cell penetrating peptides.

cSCKs are nanoparticles consisting of a hydrophobic core and a positively charged, highly functionalizable cross-linked shell. We have recently found that these nanoparticles greatly facilitate the entry of plasmid DNA and phosphorothioate 2′-*O*-methyl oligoribonucleotides into cells through a likely endocytotic mechanism mediated by the positively charged shell.[19] cSCKs are prepared in a multistep process involving the synthesis of an amphiphilic block copolymer, in this particular example, consisting of a polystyrene block linked to a poly(acrylic acid) segment, the carboxylic acids of which are then elaborated into primary amines by coupling to a monoprotected diamine, followed by deprotection. At pH 7, these amines are largely protonated, facilitating the formation of a micelle consisting of a hydrophobic polystyrene core and a hydrophilic, positively charged shell. The micelle is then stabilized by covalently cross-linking of the shell by amide formation between chains with an activated diester. In this paper, we will show how cSCKs can be used to efficiently deliver PNAs into cells *via* electrostatic complexation with a negatively charged PNA·ODN hybrid, and *via* covalent attachment of a PNA through a bioreductively cleavable disulfide bond (Figure 1). We also show that cSCKs are able to both facilitate endocytosis and endosomal release of the PNAs.

Experimental Section

Materials. All solvents and chemicals were purchased from Sigma-Aldrich and used without further purification, unless otherwise indicated. *N*-Hydroxybenzotriazole·H_2O (HOBt) and 2-(1*H*-benzotriazole-1-yl)-1,1,3,3-tetramethyluronium hexafluorophosphate (HBTU) were purchased from EMD Chemicals, Inc. The amphiphilic block copolymer, poly(acrylic acid)$_{128}$-*block*-polystyrene$_{40}$ (PAA_{128}-*b*-PS_{40}), was prepared using atom transfer radical polymerization of (protected) monomer precursors followed by deprotection, according to literature reported methods.[20] This polymer was then transformed into poly(acrylamidoethylamine)$_{128}$-*block*-polystyrene$_{40}$ ($PAEA_{128}$-*b*-PS_{40}) and used for the creation of the cSCKs, according to the literature reported sequence of procedures.[19] The pLuc705 HeLa cell line was a generous gift from Dr. R. Kole (University of North Carolina, Chapel Hill, NC). Lipofectamine 2000 was obtained from Invitrogen Co. Polyfect was purchased from Qiagen Inc. Steady-Glo Luciferase Assay reagent and CellTiter-Glo Luminescent Cell Viability Assay Kit were purchased from Promega Co. All cell culture media were purchased from Invitrogen, Inc.

Measurements. ^{1}H NMR and ^{13}C NMR spectra were recorded on a Varian 300 MHz spectrometer interfaced to a UNIX computer using Mercury software. Chemical shifts were referenced to the solvent resonance signals. IR spectra were recorded on a Perkin-Elmer Spectrum BX FT-IR system, and data were analyzed using Spectrum v2.0 software. Tetrahydrofuran-based gel permeation chromatog-

(8) Rasmussen, F. W.; Bendifallah, N.; Zachar, V.; Shiraishi, T.; Fink, T.; Ebbesen, P.; Nielsen, P. E.; Koppelhus, U. Evaluation of transfection protocols for unmodified and modified peptide nucleic acid (PNA) oligomers. *Oligonucleotides* **2006**, *16* (1), 43–57.
(9) Abes, S.; Moulton, H.; Turner, J.; Clair, P.; Richard, J. P.; Iversen, P.; Gait, M. J.; Lebleu, B. Peptide-based delivery of nucleic acids: design, mechanism of uptake and applications to splice-correcting oligonucleotides. *Biochem. Soc. Trans.* **2007**, *35* (Pt 1), 53–5.
(10) Koppelhus, U.; Shiraishi, T.; Zachar, V.; Pankratova, S.; Nielsen, P. E. Improved Cellular Activity of Antisense Peptide Nucleic Acids by Conjugation to a Cationic Peptide-Lipid (CatLip) Domain. *Bioconjugate Chem.* **2008**, *19*, 1526–1534.
(11) Reineke, T. M.; Grinstaff, M. W. Designer materials for nucleic acid delivery. *MRS Bull.* **2005**, *30* (9), 635–638.
(12) Toub, N.; Malvy, C.; Fattal, E.; Couvreur, P. Innovative nanotechnologies for the delivery of oligonucleotides and siRNA. *Biomed. Pharmacother.* **2006**, *60* (9), 607–20.
(13) Sokolova, V.; Epple, M. Inorganic Nanoparticles as Carriers of Nucleic Acids into Cells. *Angew. Chem., Int. Ed.* **2008**, *47* (8), 1382–1395.
(14) Zhang, K.; Fang, H.; Chen, Z.; Taylor, J.-S. A.; Wooley, K. L. Shape Effects of Nanoparticles Conjugated with Cell-Penetrating Peptides (HIV Tat PTD) on CHO Cell Uptake. *Bioconjugate Chem.* **2008**, *19* (9), 1880–1887.
(15) Juliano, R.; Alam, M. R.; Dixit, V.; Kang, H. Mechanisms and strategies for effective delivery of antisense and siRNA oligonucleotides. *Nucleic Acids Res.* **2008**, *36* (12), 4158–4171.
(16) Becker, M. L.; Remsen, E. E.; Pan, D.; Wooley, K. L. Peptide-derivatized shell-cross-linked nanoparticles. 1. Synthesis and characterization. *Bioconjugate Chem.* **2004**, *15* (4), 699–709.
(17) Becker, M. L.; Bailey, L. O.; Wooley, K. L. Peptide-derivatized shell-cross-linked nanoparticles. 2. Biocompatibility evaluation. *Bioconjugate Chem.* **2004**, *15* (4), 710–7.
(18) O'Reilly, R. K.; Hawker, C. J.; Wooley, K. L. Cross-linked block copolymer micelles: functional nanostructures of great potential and versatility. *Chem. Soc. Rev.* **2006**, *35* (11), 1068–83.
(19) Zhang, K.; Fang, H.; Wang, Z.; Taylor, J. S.; Wooley, K. L. Cationic shell-crosslinked knedel-like nanoparticles for highly efficient gene and oligonucleotide transfection of mammalian cells. *Biomaterials* **2009**, *30* (5), 968–77.
(20) Ma, Q.; Wooley, K. L. The preparation of t-butyl acrylate, methyl acrylate, and styrene block copolymers by atom transfer radical polymerization: precursors to amphiphilic and hydrophilic block copolymers and conversion to complex nanostructured materials. *J. Polym. Sci., Part A: Polym. Chem.* **2000**, *38* (Suppl.), 4805–4820.

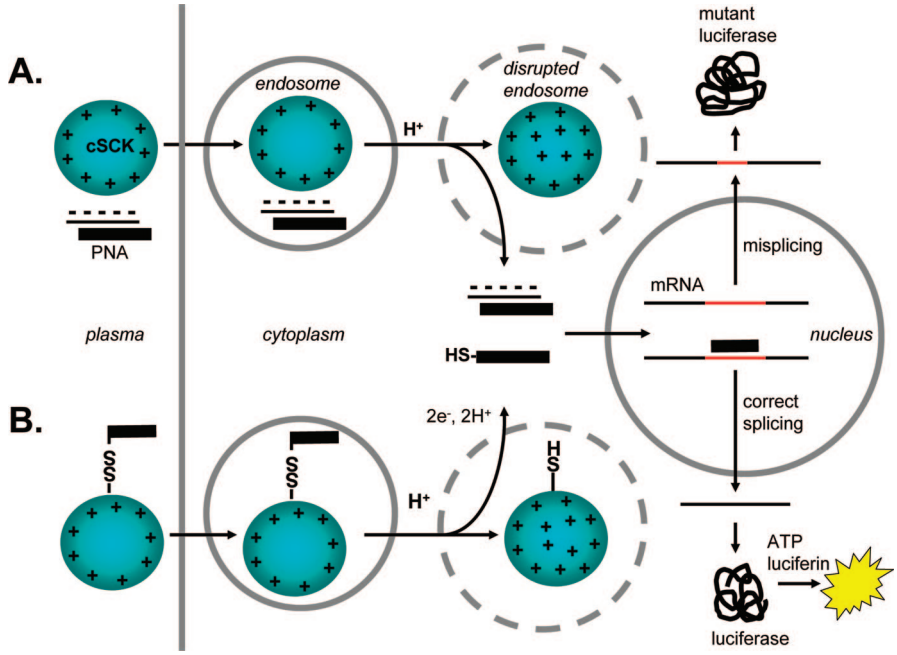

Figure 1. Strategies for the development of electrostatic and covalent-based nanoparticle agents for transfection of PNA. (A) Electrostatic system. (B) Bioreductively cleavable covalent system. At pH 7 most of the amines of the cSCK are protonated, resulting in a cationic shell that facilitates both electrostatic binding of PNA·ODN duplexes and macropinocytosis. The remaining basic groups act as a proton sponge that acquire additional protons and counterions thereby causing disruption of the endosome. In system A, this disruption causes release of the PNA·ODN into the cytoplasm from where it can translocate into the nucleus. Binding of the PNA to the mis-splicing site in the pLuc705 luciferase gene corrects the splicing which results in active luciferase which can be assayed by the production of light in the presence of luciferin. In the case of the covalently linked system B, disruption of the endosome exposes the cSCK to reducing agents which cleave the disulfide bond and cause the release of the splice-correcting PNA.

raphy (THF GPC) was conducted on a Waters Chromatography, Inc. (Milford, MA) model 1515, equipped with a Waters model 5414 differential refractometer, a Precision Detectors, Inc. (Bellingham, MA), model PD-2026 dual-angle (15° and 90°) light scattering detector and a three-column set of Polymer Laboratories, Inc. (Amherst, MA) gel mixed-bed styrene-divinylbenzene columns (PLgel 5 μm Mixed C, 500 Å, and 104 Å, 300 × 7.5 mm columns). The system was equilibrated at 35 °C in tetrahydrofuran (THF), which served as the polymer solvent and eluent (flow rate set to 1.00 mL/min). An injection volume of 200 μL was used. System calibration was performed using polystyrene standards. Data were analyzed using Precision Detectors, Inc., Discovery 32 software. *N*,*N*-Dimethylformamide-based gel permeation chromatography (DMF GPC) was conducted on a Waters system equipped with an isocratic pump model 1515, a differential refractometer model 2414 and a two-column set of Styragel HR 4 and HR 4E 5 μm DMF 7.8 × 300 mm columns. The system was equilibrated at 70 °C in prefiltered *N*,*N*-dimethylformamide (DMF) containing 0.05 M LiBr, which served as polymer solvent and eluent (flow rate set to 1.00 mL/min). Polymer solutions were prepared at concentrations of *ca.* 3 mg/mL, and an injection volume of 200 μL was used. Data collection and analysis was performed with Empower Pro software. The system was calibrated with poly(ethylene glycol) standards (Polymer Laboratories, Amherst, MA) ranging from 615 to 443,000 Da. Samples for transmission electron microscopy (TEM) measurements were diluted with a 1% phosphotungstic acid (PTA) stain (v/v, 1:1). Carbon grids were exposed to oxygen plasma treatment to increase the surface hydrophilicity. Micrographs were collected at 50000× and 100000× magnifications. Hydrodynamic diameters (D_h) and size distributions were determined by dynamic light scattering (DLS). The DLS instrumentation consisted of a Brookhaven Instruments Limited (Worcestershire, U.K.) system, including a model BI-200SM goniometer, a model BI-9000AT digital correlator, a model EMI-9865 photomultiplier, and a model 95-2 argon ion laser (Lexel Corp.) operated at 514.5 nm. Measurements were made at 25 ± 1 °C. Scattered light was collected at a fixed angle of 90°. A photomultiplier aperture of 100 μm was used, and the incident laser intensity was adjusted to obtain a photon counting of between 200 and 300 kcps. Only measurements in which the measured and calculated baselines of the intensity autocorrelation function agreed to within 0.1% were used to calculate particle size. The calculations of the particle size distributions and distribution averages were performed with the ISDA software package (Brookhaven Instruments Company). All determinations were repeated 5 times.

PNA Synthesis. All PNAs and conjugates were synthesized on an Expedite 8900 PNA synthesizer on 2 μmol of Fmoc-PAL-PEG-PS according to the standard automated Fmoc PNA synthesis procedure utilizing commercial mono-

mers (Panagene Inc., Korea). Following the final step of automated synthesis the resin was washed with dry DMF (2 × 3 mL) and dry CH_2Cl_2 (2 × 3 mL), followed by drying under a stream of N_2. The resin was then shaken in a vial with trifluoroacetic acid (300 μL) and *m*-cresol (100 μL) at room temperature for 2 h to release and deprotect the PNA. The solution was filtered from the resin, and added into ice-cold Et_2O (5 mL) and kept at 4 °C for 1 h. The resulting precipitate was collected by centrifugation and purified by reverse-phase HPLC on a Varian Microsorb-MV C18 column (300 Å) with buffer A [0.1% TFA in H_2O] and buffer B [0.1% TFA in CH_3CN] on a Beckman System Gold instrument equipped with a UV−vis array detector. The fractions were collected and concentrated to dryness in a SpeedVac (Savant) and characterized by UV−vis, and MALDI-TOF was carried out on a PerSpective Voyager mass spectrometer with α-cyano-4-hydroxycinnamic acid as the matrix and insulin as the internal reference.

PNA. The PNA H-CCTCTTACCTCAGTTACA-NH_2 was synthesized and purified by the general procedure described above. MALDI: average $[M + H]^+$ expected 4766.6, found 4764.4.

HO_2C-PNA. Following automated PNA synthesis of H-CCTCTTACCTCAGTTACA-NH_2 and washing, but prior to cleavage and deprotection, the resin was removed from the column and shaken in piperidine (1 mL) and dry DMF (4 mL) for 30 min. The resin was then filtered and washed with dry DMF (2 × 3 mL) and dry CH_2Cl_2 (2 × 3 mL) and dried under a stream of N_2. The resin was removed from the column and suspended in dry DMF (100 μL) to which succinic anhydride (20 μmol, 2.0 mg) was added, followed by diisopropylethylamine (20 μmol, 3.5 μL). The mixture was shaken for 12 h before cleavage and deprotection. MS: average $[M + H]^+$ expected 4866.7, found 4867.8.

HO_2C-SS-PNA. Following automated PNA synthesis of H-CCTCTTACCTCAGTTACA-NH_2 and washing, but prior to cleavage and deprotection, the resin was removed from the column and shaken in piperidine (1 mL) and dry DMF (4 mL) for 30 min. The resin was then filtered and washed with dry DMF (2 × 3 mL) and dry CH_2Cl_2 (2 × 3 mL) and dried under a stream of N_2. To a suspension of the resin in dry DMF (100 μL) was added 3,3′-dithiodipropionic acid (20 μmol, 4.2 mg) (Aldrich), followed by 4-dimethylaminopyridine (20 μmol, 2.4 mg) and *N*,*N*′-dicyclohexylcarbodiimide (20 μmol, 4.1 mg). The mixture was shaken for 12 h before filtration and final deprotection. MALDI: average $[M + H]^+$ expected 4958.9, found 4960.0.

HO_2C-SS-PNA-Lys(FITC). Following automated synthesis of H-CCTCTTACCTCAGTTACA-L-Lys(εMtt)-NH_2 using *N*-α-Fmoc-*N*-ε-4-methyltrityl-L-lysine (AnaSpec) but prior to Fmoc deprotection, the resin was removed from the column and treated multiple times with 2% trifluoroacetic acid in methylene chloride (5 mL) until the solution was colorless to selectively remove the Mtt group. The resin was then washed with dry DMF (2 × 3 mL) and dry CH_2Cl_2 (2 × 3 mL) and dried under a stream of N_2. To a suspension of the resin in dry DMF (100 μL) was added FITC (fluorescein isothiocyanate, isomer I, Aldrich) (20 μmol, 7.8 mg), followed by addition of diisopropylethylamine (20 μmol, 3.5 μL) and shaking for 12 h. The resin was then washed with dry DMF (2 × 3 mL) and dry CH_2Cl_2 (2 × 3 mL), followed by drying under a stream of N_2 prior to coupling with 3,3′-dithiodipropionic acid as described above.

General Procedure for the Conjugation of PNA to $PAEA_{128}$-*b*-PS_{40} and formation of micelles. PNA (0.68 μmol) was dissolved in dry DMSO (300 μL), to which 20 μL of DMSO solution containing 4 equiv of 1:1 (mol:mol) HBTU/HOBt was added to activate the carboxylic termini of the PNAs. After 30 min, 0, 9, 92 and 185 μL of the activated PNA solution was added to 4 vials, each containing 2 mg of $PAEA_{128}$-*b*-PS_{40} and 9 μL of DIPEA (4 equiv to the polymer NH_2 residues) in 386 μL of DMSO. The vials were then sealed, and the solutions were stirred for 48 h. Following the allocated reaction times, DMSO was added to each vial to give a final volume of 1 mL, and the mixtures were transferred to dialysis tubing (MWCO: 15 kDa) and dialyzed against 300 mM NaCl solution for 4 days, then nanopure water (18 MΩ·cm) for 2 days, to give the micelle precursor for the cSCK and cSCK-PNA conjugates. The final polymer concentration was 0.70 mg/mL. The number of PNA per polymer was calculated to be 0, 0.1, 1 and 2, based on UV−vis measurement of the PNA absorption at 260 nm. For the preparation of cSCK(Alexa Fluor 633)-SS-PNA(FITC)$_2$, Alexa Fluor 633 succinimidyl ester (Invitrogen) was added to the reaction mixture following the addition of HO_2C-SS-PNA(FITC).

General Procedure for the Cross-Linking of cSCK and cSCK-PNA Micelles. The diacid cross-linker (5.0 mg, 14 μmol) was activated by mixing with 2.2 equiv of HOBt/HBTU (4 mg/12 mg, 1:1, mol:mol) in DMF (400 μL) and stirring for 1 h. The activated cross-linker solution (0.67 μmol/19 μL, equivalent to 5% of polymer NH_2 groups) was then added slowly with stirring to 2.9 mL of the aqueous micelle solutions (∼0.7 mg/mL), which had been adjusted to pH 8.0, using 1.0 M aqueous sodium carbonate, and cooled to 0 °C, using an ice bath. The reaction mixture was stirred overnight, and was then transferred to dialysis tubing (8 kDa MWCO) and dialyzed against nanopure water (18 MΩ·cm) for 2 days. Clear solutions containing the cSCKs and cSCK-PNA conjugates with a final polymer concentration of 0.65 mg/mL were obtained.

Cell Culture. cSCK-mediated PNA delivery was evaluated on pLuc705 HeLa cells. Cells were maintained in DMEM containing 10% FBS, streptomycin (100 μg/mL), penicillin (100 units/mL), G418 (100 μg/mL) and hygromycin B (100 μg/mL) at 37 °C in a humidified atmosphere with 5% CO_2.

Splice Correction Assay. pLuc705 HeLa cells were seeded in a 96-well microtiter plate at a density of 2×10^4 cells/well and cultured for 24 h in 100 μL of DMEM containing 10% FBS. For delivery of covalent cSCK-PNA conjugates, pLuc705 cells were treated with 100 μL/well the cSCK-PNA solution in DMEM medium (10% FBS) for 24 h. For PNA/ODN heteroduplex (electrostatically associated)

delivery, PNA·ODN duplexes were formed prior to addition to the cell plates. Formation of PNA·ODN heteroduplexes was performed by gradual mixing of PNA (H-CCTCTTAC-CTCAGTTACA-NH_2) and complementary (underlined) ODN (5′-AATATGTAACTGAGGTA-3′). The PNA·ODN heteroduplex was then incubated with Lipofectamine 2000, Polyfect or cSCK in 20 μL of OPTI-MEM for 15 min, before addition to pLuc705 cell wells containing 80 μL of fresh culture medium. After 24 h incubation, 100 μL of Steady-Glo Luciferase assay reagent were added. The contents were mixed and allowed to incubate at room temperature for 10 min to stabilize luminescence. Signals were recorded on a Luminoskan Ascent luminometer (Thermo Scientific) with an integration time of 1 s per well.

Cytotoxicity Assay. Cytotoxicities of the cSCK and cSCK-PNA conjugates were examined by CellTiter-Glo Luminescent Cell Viability Assay (Promega Co.). HeLa cells were seeded in a 96-well plate at a density of 2×10^4 cells/well and cultured for 24 h in 100 μL of DMEM containing 10% FBS. Thereafter, the medium was replaced with 100 μL of fresh medium containing various concentrations of cSCKs, cSCK-PNA conjugates, Polyfect, Lipofectamine 2000 (positive controls), or no additive (negative control). After 24 h incubation at 37 °C, 100 μL of CellTiter-Glo reagent was added. The contents were mixed and the plate was allowed to incubate at room temperature for 10 min to stabilize the luminescence signals. Luminescence intensities were recorded on a Luminoskan Ascent luminometer (Thermo Scientific) with an integration time of 1 s per well. The relative cell viability was calculated by the following equation where $\text{luminescence}_{(\text{negative control})}$ is in the absence of particles and where $\text{luminescence}_{(\text{sample})}$ is in the presence of particles.

$$\text{cell viability (\%)} = (\text{luminescence}_{\text{sample}}/\text{luminescence}_{\text{negative control}}) \times 100$$

RT-PCR. pLuc705 HeLa cells were seeded in a 24-well plate at a density of 5×10^4 cells/well and treated as described above for the splice correction assay. Total RNA was isolated using Trizol reagent (Invitrogen, Inc.) following the manufacturer's instructions. cDNA was synthesized with SuperScript II (Invitrogen Inc.), after TURBO DNase (Ambion, Inc.) treatment. The cDNA was then used as a template for PCR, which was carried out using GoTaq Flexi DNA Polymerase (Promega, Inc.). Primers for PCR were as follows: forward primer, 5′-TTGATATGTGGATTTC-GAGTCGTC-3′; reverse primer, 5′-TGTCAATCAGAGT-GCTTTTGGCG-3′. Forward primer was labeled by [γ-^{32}P]-ATP with T4 Polynucleotide Kinase. The PCR program was as follows: (95 °C, 2 min) × 1 cycle, (95 °C, 0.5 min; 55 °C, 0.5 min; 72 °C, 0.5 min) × 24 cycles, (72 °C, 5 min) × 1 cycle. The PCR products were analyzed on 8% native polyacrylamide gel with 1 × TBE buffer. Gel images were scanned by a BioRad Phosphorimager and analyzed by Quantity One software (Bio-Rad Co.).

Fluorescence Confocal Microscopy. HeLa cells (5×10^5) were plated in 35 mm MatTek glass bottom microwell dishes (MatTek Co.) 24 h prior to transfection. At the time of transfection, the medium in each dish was replaced with 2 mL of fresh medium. Then, cSCK(Alexa Fluor 633)-SS-PNA(FITC)$_2$ (80 μL) was added. The dishes were then returned to the incubator to incubate at 37 °C for 1 or 24 h. Each dish was washed 3× with PBS buffer and viewed under bright field and fluorescence conditions using a Leica TCS SP2 inverted microscope, with excitation by an Ar laser (488 nm) and a HeNe laser (633 nm).

Results and Discussion

PNA Transfection Strategies. We investigated two strategies for introducing PNAs into cells that make use of the unique properties of the cSCKs (Figure 1). The cSCKs were designed to resemble histone core particles in their nanoscopic size, positively charged surfaces, and DNA packaging ability, while also possessing characteristics that would lead to their use as synthetic vectors for gene delivery. We have recently shown that cSCKs efficiently deliver negatively charged plasmid and oligonucleotides into cells through an endocytotic mechanism, most likely macropinocytosis.[19] Therefore, in this current study, the first strategy was to deliver PNA through electrostatic complexation with the cSCK by hybridizing it to a negatively charged complementary ODN (Figure 1A). The second strategy was to deliver the PNA through covalent attachment of the PNA to the cSCK (Figure 1B). Because the cSCKs are large (about 10 nm in diameter) relative to the PNAs, a covalently attached PNA might be engulfed by the nanoparticle, thereby being unable to enter the nucleus and/or bind to the splice correction site. In addition, it was recognized that, should the cSCKs be trapped in intracellular compartments, having an ability to disconnect the PNA from the cSCK nanostructure would be important. We, therefore, decided to attach the PNA *via* a bioreductively cleavable disulfide linkage. This linkage is expected to be stable in serum, but upon exposure to the cytosol be reduced, thereby liberating the PNA.

Design and Synthesis of the cSCK and Constructs. The particular cSCK was chosen for its ability to efficiently transfect negatively charged plasmid DNA and 2′-*O*-methyl phosphorothioate oligoribonucleotides.[19] The cSCK was synthesized by micellization and cross-linking of a block copolymer consisting of a 40-mer polystyrene block and a 128-mer poly *N*-(2-aminoethyl)acrylamide block (Figure 2). The block copolymer was prepared by sequential atom transfer radical polymerization of protected monomers followed by three steps of postpolymerization modifications. The lengths of the blocks were estimated from GPC and ^{1}H NMR spectroscopy after each step of polymerization. Micellization was carried out by rapid dilution of a DMSO solution of the block copolymer into water at pH 6. The shell is then cross-linked by the addition of an activated diester. The cSCKs were characterized by DLS, TEM and ζ potential measurements. They were found to be of a globular morphology having a number-average diameter of approximately 10 nm (TEM) and with a ζ potential value of

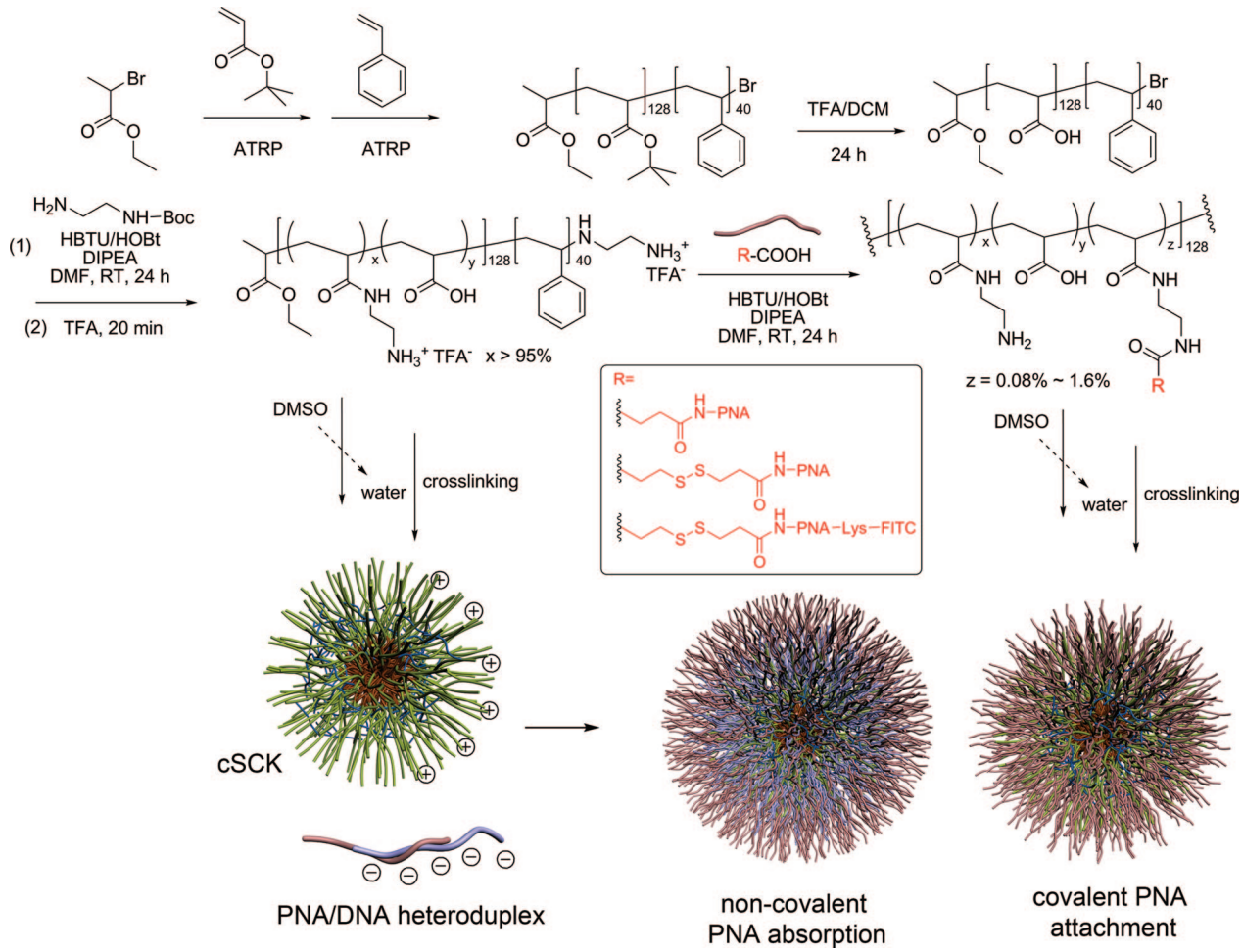

Figure 2. Synthesis of the electrostatic and covalent-based nanoparticle transfection agents. The starting material consists of a block copolymer having a hydrophobic styrene block and a hydrophilic primary amine-bearing block ($PAEA_{128}$-*b*-PS_{40}). Micellization of this block copolymer by dialysis of its DMSO solution against water followed by cross-linking with an activated diester affords the cSCKs. Subsequent electrostatic association with PNA·ODN gives the cSCK carrying PNA via noncovalent PNA absorption. To make the covalently linked cSCK-SS-PNA nanoparticles, the block copolymer was coupled to a carboxy-terminated disulfide-linked PNA and then micellized and cross-linked.

21.3 mV. From TEM measurement of the particle core size, each cSCK is estimated to be comprised of *ca*. 60 chains, or *ca*. 7700 amines.

The cSCKs bearing a covalently linked PNA were prepared by linking of a carboxy terminal PNA with the block copolymer, facilitated by HBTU/HOBt, prior to micellization. The PNAs were coupled so as to give 0.1, 1 or 2 PNAs/polymer chain and purified by extensive dialysis against 300 mM NaCl solution, and then against nanopure water. The amount of PNA per chain was calculated from the estimated molar absorption coefficients for the PNA. The polymer-PNA conjugates were micellized by the same procedure as for the cSCK and similarly characterized by DLS, TEM and ζ potential measurement. They were found to be indistinguishable in size and surface charge from the non-PNA-conjugated cSCKs. Three types of construct were prepared: one with a nonbioreductively cleavable linker, cSCK-PNA; one with a bioreductively cleavable disulfide-bearing linker, cSCK-SS-PNA; and one with an Alexa Fluor 633 label on the cSCK linked to a FITC labeled PNA *via* a disulfide linker, cSCK(Alexa Fluor 633)-SS-PNA$(FITC)_2$.

PNA Transfection Efficiency Assays. To rapidly and quantitatively assay for the effectiveness of our two PNA transfection strategies, we adopted the luciferase splice correction assay developed by Kole and co-workers[21] and later used to evaluate PNAs.[8] This assay relies on a luciferase gene (pLuc705) that results in a longer, mis-spliced mRNA that encodes a defective luciferase (Figure 1). In the presence of a PNA complementary to the aberrant splice site, correct splicing is restored, resulting in a shorter mRNA and an active luciferase. The extent to which splicing is corrected can then be monitored easily in a high throughput fashion, by measuring the light produced by the luciferase enzyme in the presence of luciferin. The light output is, thus, a

(21) Kang, S. H.; Cho, M. J.; Kole, R. Up-regulation of luciferase gene expression with antisense oligonucleotides: implications and applications in functional assay development. *Biochemistry* **1998**, *37* (18), 6235–9.

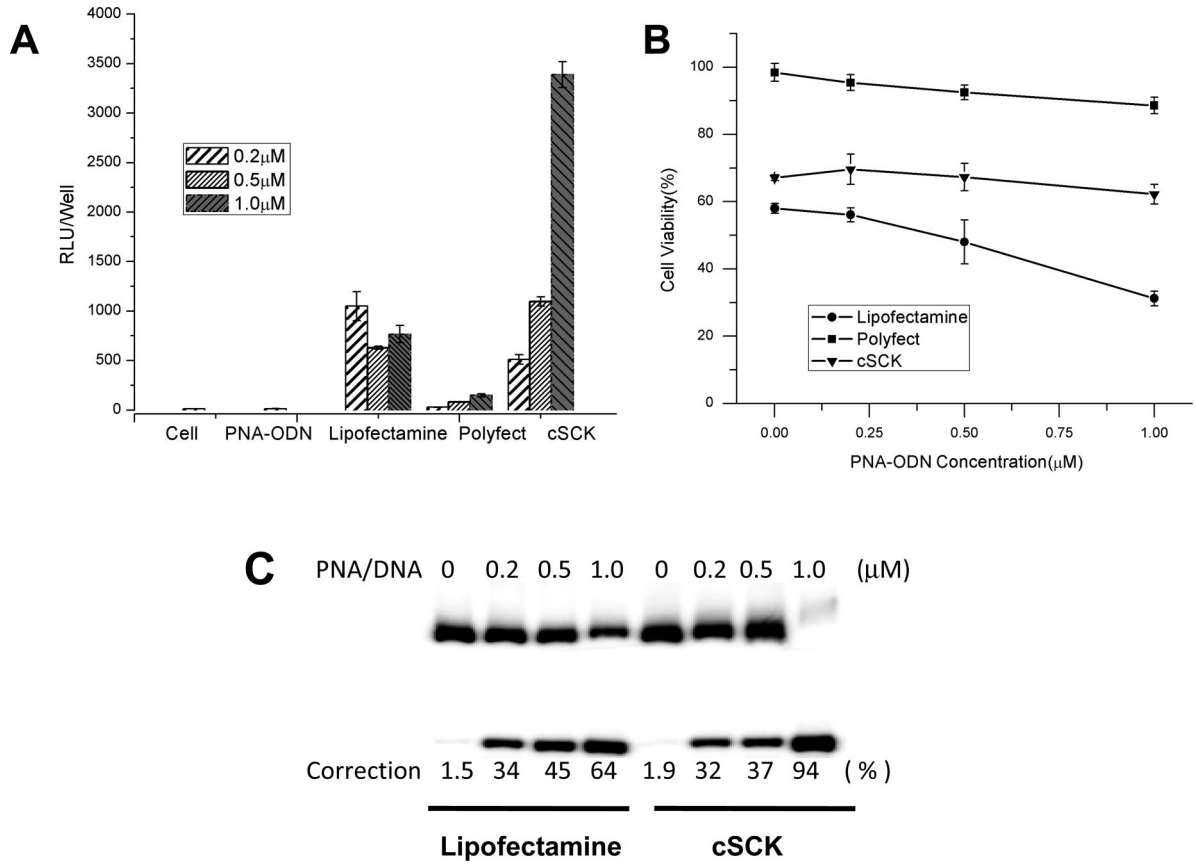

Figure 3. Bioactivity and cytotoxicity of electrostatically mediated PNA·ODN delivery by cSCKs and conventional agents. Splice-correcting PNA that was hybridized to an equimolar amount of partially complementary ODN and then was mixed with 10 μg/mL of Lipofectamine 2000, 20 μg/mL Polyfect, or 20 μg/mL cSCK to give 0.2, 0.5, 1 μM final concentration of PNA. (A) pLuc705 HeLa cells were incubated with transfection agent for 24 h, and then assayed for PNA bioactivity *via* luciferase activity. (B) Cell viability was assayed by an ATP assay and shown as a percentage of the viability of the control cells. (C) Percentage splice correction by an RT-PCR assay for the different PNA·ODN concentrations. The upper band corresponds to a 268 bp fragment from mis-splicing, while the lower band corresponds to a 142 bp fragment from correct splicing.

function of the transfection efficiency and cytotoxicity. The extent of splice correction can also be directly and quantitatively assayed by RT-PCR. To evaluate the cytotoxicity of the agents, we relied on cell viability measurements based on quantification of the amount of ATP produced by metabolically active cells.

Transfection of PNA·ODN Hybrids by cSCKs. Cationic transfection agents have been developed that can efficiently deliver negatively charged nucleic acids into cells in culture, but cannot deliver PNAs because of their lack of charge. A simple solution to this problem is to hybridize the PNA to a partially complementary oligodeoxynucleotide (ODN) prior to transfection with a cationic agent, such as the cationic lipid Lipofectamine.[6] Many factors have been found to affect the bioactivity of pLuc705 PNA·ODN hybrids, such as the length, sequence, and complementarity of the ODN, the PNA/ODN ratio, the ratio of the PNA·ODN to the cationic transfection agents, the type of cationic transfection agent (Lipofectamine or PEI), and their cytotoxicity.[8] We selected the PNA·ODN hybrid found to have the highest bioactivity in that study and compared its bioactivity in the presence of cSCK to Lipofectamine 2000, and Polyfect, a cationic dendrimer[22] (Figure 3A). At a low concentration of PNA·ODN 0.2 μM, the bioactivity was two times higher with Lipofectamine 2000 than with cSCK, both of which were better than Polyfect. Increasing the amount of PNA·ODN to 1.0 μM decreased slightly the bioactivity with Lipofectamine 2000, perhaps due to an increase in cytotoxicity, as indicated by a drop in cell viability from 58% to 30% (Figure 3B). In contrast, increasing the PNA·ODN concentration 5-fold from 0.2 μM to 1.0 μM, increased the bioactivity about 7-fold when cSCK was used, without increasing the cytotoxicity. The bioactivity for the 1 μM PNA·ODN in the presence of the cSCK was about 5-fold greater than observed for Lipofectamine 2000. Polyfect was not found to be effective for PNA·ODN delivery at any concentration even though its cytotoxicity is lower than Lipofectamine 2000 and cSCK.

The correlation between bioactivity in the luciferase assay and splice correction was investigated by RT-PCR analysis

(22) Tang, M. X.; Redemann, C. T.; Szoka, F. C., Jr. *In vitro* gene delivery by degraded polyamidoamine dendrimers. *Bioconjugate Chem* **1996**, *7* (6), 703–14.

of the luciferase mRNA (Figure 3C). Whereas increasing the PNA·ODN concentration from 0.2 μM to 1.0 μM in the presence of 10 μg/mL of Lipofectamine 2000 resulted in a slight decrease in bioactivity, the amount of splicing increased 2-fold from 34% to 64%. This result is consistent with the greater cytotoxicity at the higher PNA·ODN concentrations, which would reduce the number of viable cells and hence the light output (bioactivity). In contrast, the increase in bioactivity with increasing PNA·ODN concentration in the presence of 20 μg/mL of cSCK correlated better with the amount of splice correction, consistent with a minimal change in cytotoxicity. Changing the concentration of PNA·ODN 2-fold from 0.5 μM to 1.0 μM increased the bioactivity about 3-fold, while the amount of splice correction increased 2.6-fold. The nonlinear increase in splice correction with PNA·ODN concentration may reflect changes in the cell penetrating properties of the cSCK when loaded with increasing amounts of PNA·ODN. It may also be due to a reduced binding affinity of the cSCK for the PNA·ODN at higher loadings, due to a reduction in the number of excess positive charges that would facilitate release of the PNA·ODN in the cell.

The optimal bioactivity for transfection with the cSCK results from a delicate balance between transfection efficiency and cytotoxicity (Figure 4). The bioactivity of 0.5 μM PNA·ODN increased from 10 to 1200 RLU as the concentration of the cSCK was increased from 0 to 30 μg/mL, then dropped on going to 40 μg/mL (Figure 4A). The cytotoxicity increased over these concentrations, with the cell viability dropping almost linearly from 90% at 10 μg/mL to about 20% at 40 μg/mL of cSCK (Figure 4B). The large increase in bioactivity on going from 10 μg/mL to 20 μg/mL may be indicative of the capacity of the cSCK to bind to 0.5 μM PNA·ODN, or may be due to a change in size or charge that facilitated cell entry. The leveling off of the bioactivity at 30 μg/mL might then be due to an otherwise further increase in transfection by the cytotoxic effect, which then dominates at 40 μg/mL. The optimal transfection conditions in terms of bioactivity and cell viability would, therefore, appear to be between 10 and 20 μg/mL with 0.5 μM PNA·ODN.

Synthesis of the Covalently Linked cSCKs. The second transfection system that we explored involved covalent attachment of the PNA to the cSCK *via* a bioreductively cleavable linker. We chose the disulfide linkage because it has been found to be relatively stable in serum, but easily cleaved under the reducing conditions found inside cells and has been used to deliver PNAs conjoined to other delivery agents.[23,24] PNAs were covalently linked to the block copolymer prior to micelle formation and cross-linking in a 1:1 and 2:1 ratio. The amount of PNA bound could be assayed by the UV absorptivity at 260 nm (Figure 5A). Treatment of the cSCK-SS-PNA with DTT followed by dialysis removed 77% of the PNA, as judged by the decrease in absorbance at 260 nm (Figure 5B). TEM of cSCKs and cSCKs conjugated with increasing amounts of PNAs showed no noticeable differences in size, ruling out any size effects on the efficiency of cell uptake and subsequent bioactivity (Figure 5C,D).

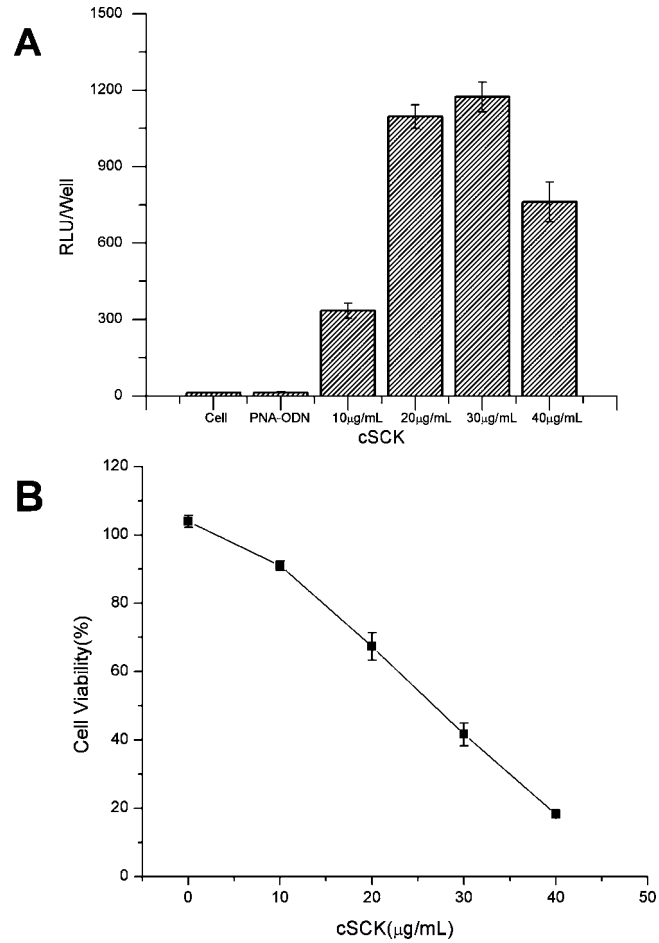

Figure 4. Relative cellular luciferase antisense activity and cytotoxicity in HeLa pLuc705 cells of cSCK-PNA·ODN complexes. Cells were incubated with 0.5 μM PNA/ODN hybrids complexed to the indicated amount of cSCK. (A) PNA bioactivity as measured by luciferase activity. (B) Cell viability.

Transfection of PNAs Covalently Linked to cSCKs. We determined the bioactivity of the bioreductively cleavable cSCK-SS-PNA and cSCK-SS-PNA_2 with one and two PNAs/chain, respectively, in comparison to the noncleavable cSCK-PNA by the splice correction assay. Both cSCKs with 1 and 2 PNAs/chain showed comparable bioactivity at 0.2 and 0.5 μM PNA concentration (Figure 6A). The cSCK with one PNA/chain showed significantly less bioactivity, however, at 1 μM PNA concentration compared to the one with two PNAs/chain. The 3-fold lower bioactivity of cSCK-SS-PNA than cSCK-SS-PNA_2 at 1 μM PNA can be explained in part

(23) Koppelhus, U.; Awasthi, S. K.; Zachar, V.; Holst, H. U.; Ebbesen, P.; Nielsen, P. E. Cell-dependent differential cellular uptake of PNA, peptides, and PNA-peptide conjugates. *Antisense Nucleic Acid Drug Dev.* **2002**, *12* (2), 51–63.

(24) Reshetnyak, Y. K.; Andreev, O. A.; Lehnert, U.; Engelman, D. M. Translocation of molecules into cells by pH-dependent insertion of a transmembrane helix. *Proc. Natl. Acad. Sci. U.S.A.* **2006**, *103* (17), 6460–5.

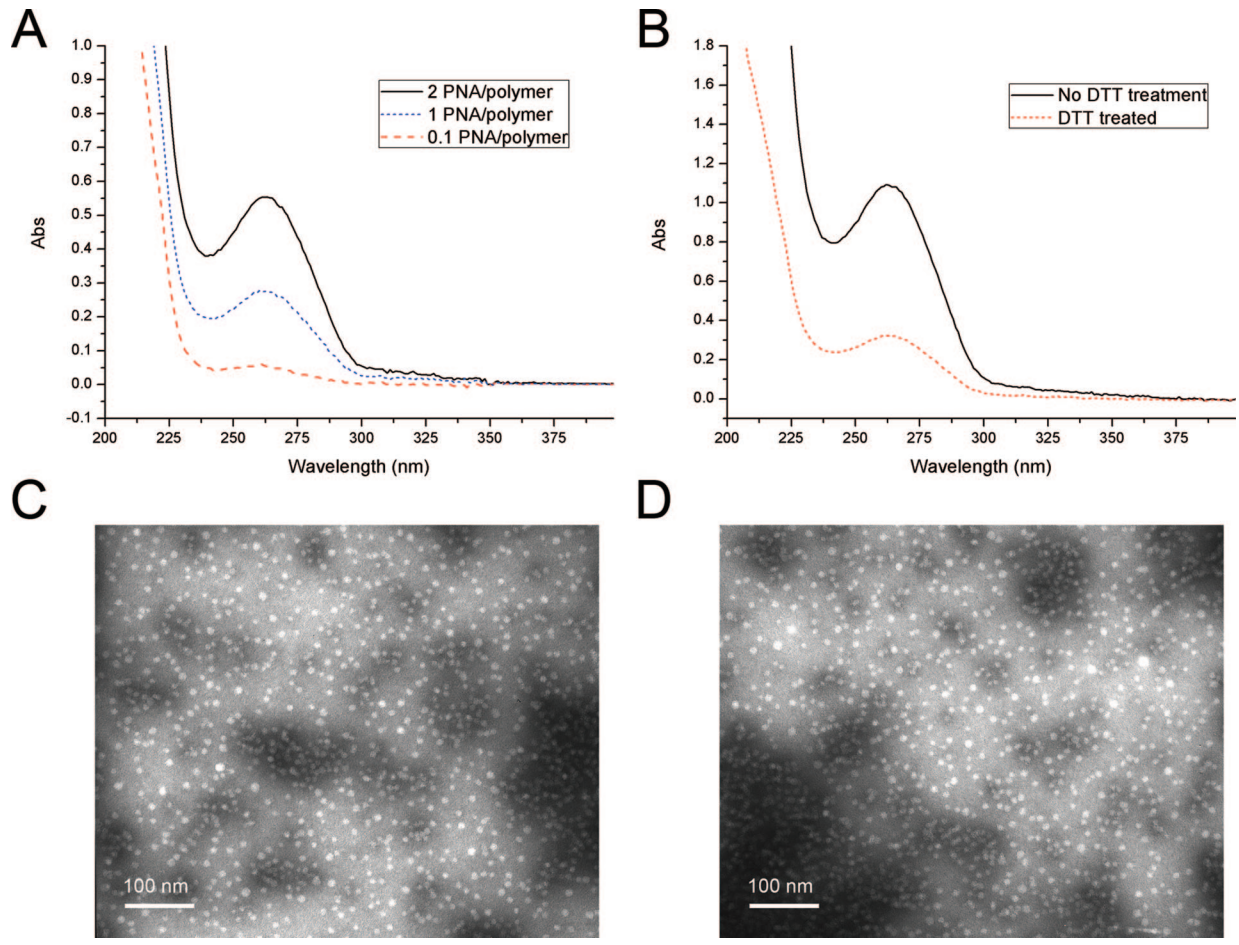

Figure 5. (A) UV characterization of the cSCK-PNA conjugates. (B) UV assay before and after reductive cleavage of the disulfide with DTT and extensive dialysis. TEM images of cSCK-SS-PNAs at (C) 2 PNA/polymer chain and (D) 0.1 PNA/polymer chain.

by the higher cytotoxicity of the 2-fold higher concentration of the cSCK-SS-PNA (48 μg/mL) needed to deliver 1 μM PNA (Figure 6B). It is not clear, however, why the bioactivity is the same for 0.5 μM PNA concentration, when the 24 μg/mL concentration of cSCK-SS-PNA is much more toxic than the 12 μg/mL concentration needed for cSCK-SS-PNA_2. Splicing correction with cSCK-SS-PNA_2 is more efficient at 1 μM PNA than at 0.5 μM PNA (85% vs. 53%) (Figure 6C) but comes at the expense of higher cytotoxicity (40% viability vs 80% viability, respectively) (Figure 6B).

Effect of Endosome Disrupting Agents on Bioactivity. It has been found that the antisense activity of PNA conjugated with cell penetrating peptides such as the TAT peptide or Arg_9 is significantly augmented by chloroquine, calcium ions, or by photochemical internalization (PCI) using photosensitizers, all of which are known to promote endosome disruption.[25−27] Since it was likely that the cSCKs were also entering cells by an endocytotic mechanism, we were interested to see whether or not these agents would also enhance the bioactivity of the cSCK-PNA conjugates. The pLuc HeLa cells were, therefore, treated with cSCK-SS-PNA conjugates in the presence or absence of 100 μM chloroquine in comparison to PNA-Arg_9 (Figure 7). As expected, chloroquine greatly enhanced the bioactivity of PNA-Arg_9 by 2 orders of magnitude. On the other hand, the cSCK-SS-PNAs were orders of magnitude more active than PNA-Arg_9 and chloroquine had little (2-fold) or no effect on the activity of cSCK-SS-PNA_2 at 0.2 and 0.5 μM PNA, respectively. In contrast, the noncleavable cSCK-PNA showed much less activity that was also not enhanced by chloroquine. One interpretation of these results is that the cSCK facilitates not only endocytosis but also endosomal escape of the PNA and/or the PNA-cSCK conjugate, without the need for chloroquine. The lower activity of the noncleavable cSCK-PNA suggests either that the cSCK-PNA is not able to escape or

(25) Hallbrink, M.; Oehlke, J.; Papsdorf, G.; Bienert, M. Uptake of cell-penetrating peptides is dependent on peptide-to-cell ratio rather than on peptide concentration. *Biochim. Biophys. Acta* **2004**, *1667* (2), 222–8.

(26) Abes, S.; Williams, D.; Prevot, P.; Thierry, A.; Gait, M. J.; Lebleu, B. Endosome trapping limits the efficiency of splicing correction by PNA-oligolysine conjugates. *J. Controlled Release* **2006**, *110* (3), 595–604.

(27) Shiraishi, T.; Nielsen, P. E. Enhanced delivery of cell-penetrating peptide-peptide nucleic acid conjugates by endosomal disruption. *Nat. Protoc.* **2006**, *1* (2), 633–6.

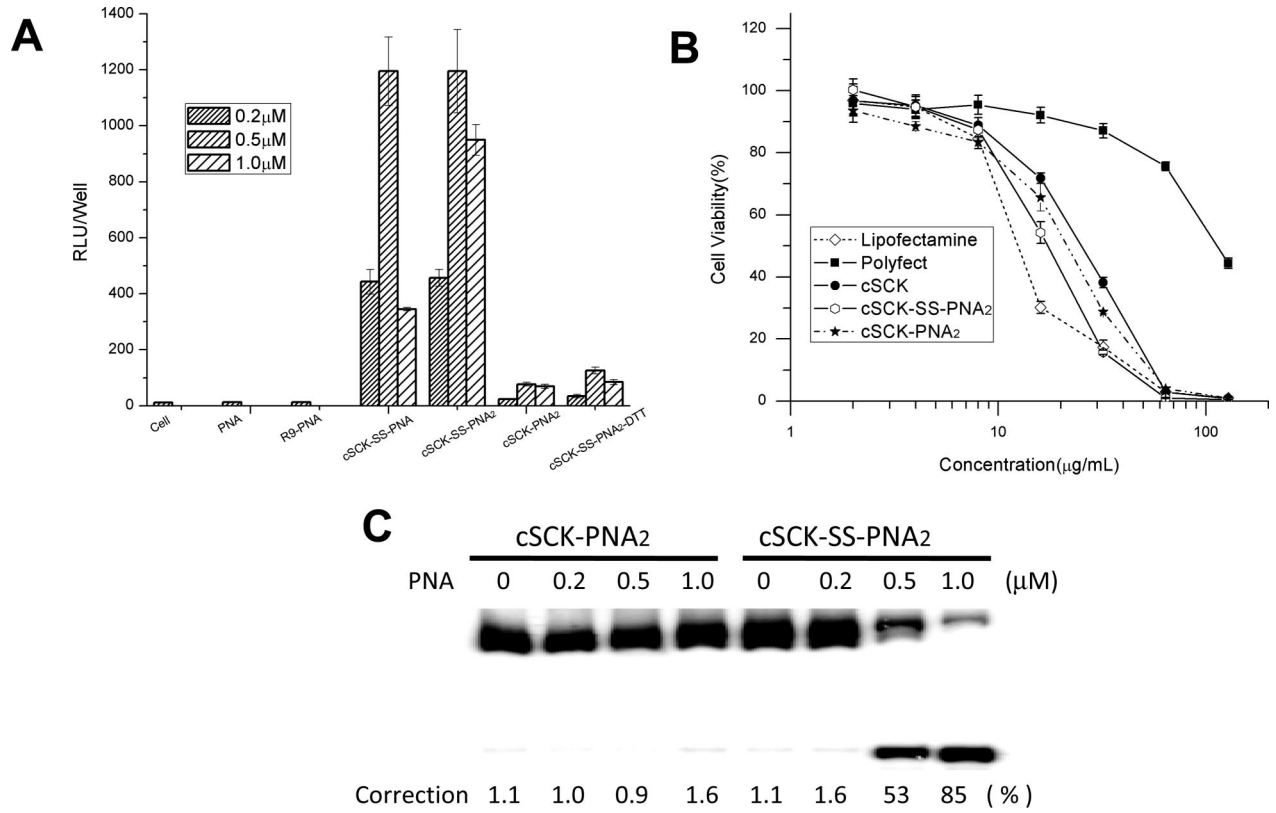

Figure 6. Splice correcting ability and cell viability of covalently linked cSCKs. (A) Splice correction efficiency of the bioreductively cleavable cSCK-SS-PNA and cSCK-SS-PNA_2 containing 1 and 2 PNAs/chain respectively and the noncleavable cSCK-PNA as a function of total PNA concentration. For a PNA concentration of 0.5 μM, the cSCK-SS-PNA_2 concentration was 12 μg/mL. (B) Cell viability as a function of concentration of the delivery agent in μg/mL. (C) Splice correction efficiency for cSCK-PNA and cSCK-SS-PNA_2.

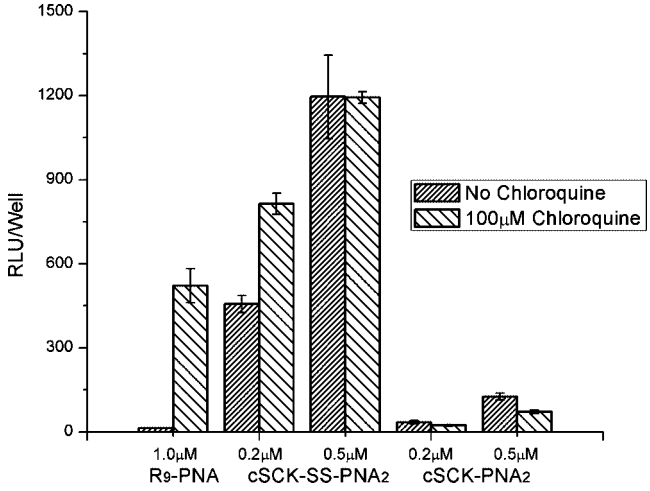

Figure 7. Effect of endosomal disrupting agents on PNA bioactivity as measured by luciferase activity. Cells were treated with 1 μM Arg_9-PNA, with 0.2 or 0.5 μM PNA from cSCK-SS-PNA_2, or with cSCK-PNA in the presence or absence of 100 μM chloroquinone.

that the cSCK-PNA is not able to enter the nucleus and/or bind to the RNA due to inaccessibility of the PNA in the shell.

Tracking cSCK Mediated PNA Delivery and Release Inside Cells. To track the intracellular path of the cSCK-SS-PNA_2 and its bioreductive cleavage products, we prepared a dual fluorescently labeled particle. The cSCK was labeled with Alexa Fluor 633 and the PNA was labeled at the ε-amino group of a carboxy terminal lysine with fluorescein isothiocyanate (FITC). The pLuc705 HeLa cells were incubated with the dual labeled cSCK(Alexa Fluor)-SS-$PNA(FITC)_2$ and examined by confocal microscopy after 1 and 24 h (Figure 8). After 1 h, cSCK and PNA fluorescence were colocalized and concentrated near the membrane surface (Figure 8B). After 24 h, cSCK fluorescence was exclusively concentrated in endosomal and/or lysosomal-like vesicles, whereas PNA fluorescence was observed in the nucleus as well as being partially colocalized with the cSCK fluorescence in the vesicles (Figure 8A). Transfection following reductive cleavage with DTT and dialysis shows only the cSCK fluorescence localized in vesicles, and little PNA fluorescence (Figure 8C). We interpret these data to support a model (Figure 1B) in which a cSCK-SS-PNA binds to the membrane surface and is then slowly endocytosed. Endosomal acidification then causes cSCK-mediated destabilization of the endosome and exposes the cSCK-SS-PNA to cytoplasmic reducing environment, causing release of the PNA, which then binds to the RNA mis-splicing site in the nucleus. The destabilization is not sufficient, however, to enable release of the cSCK, which remains trapped in the endosomes, or of sufficient duration to allow all of the PNA to be bioreductively cleaved and escape from the endosome.

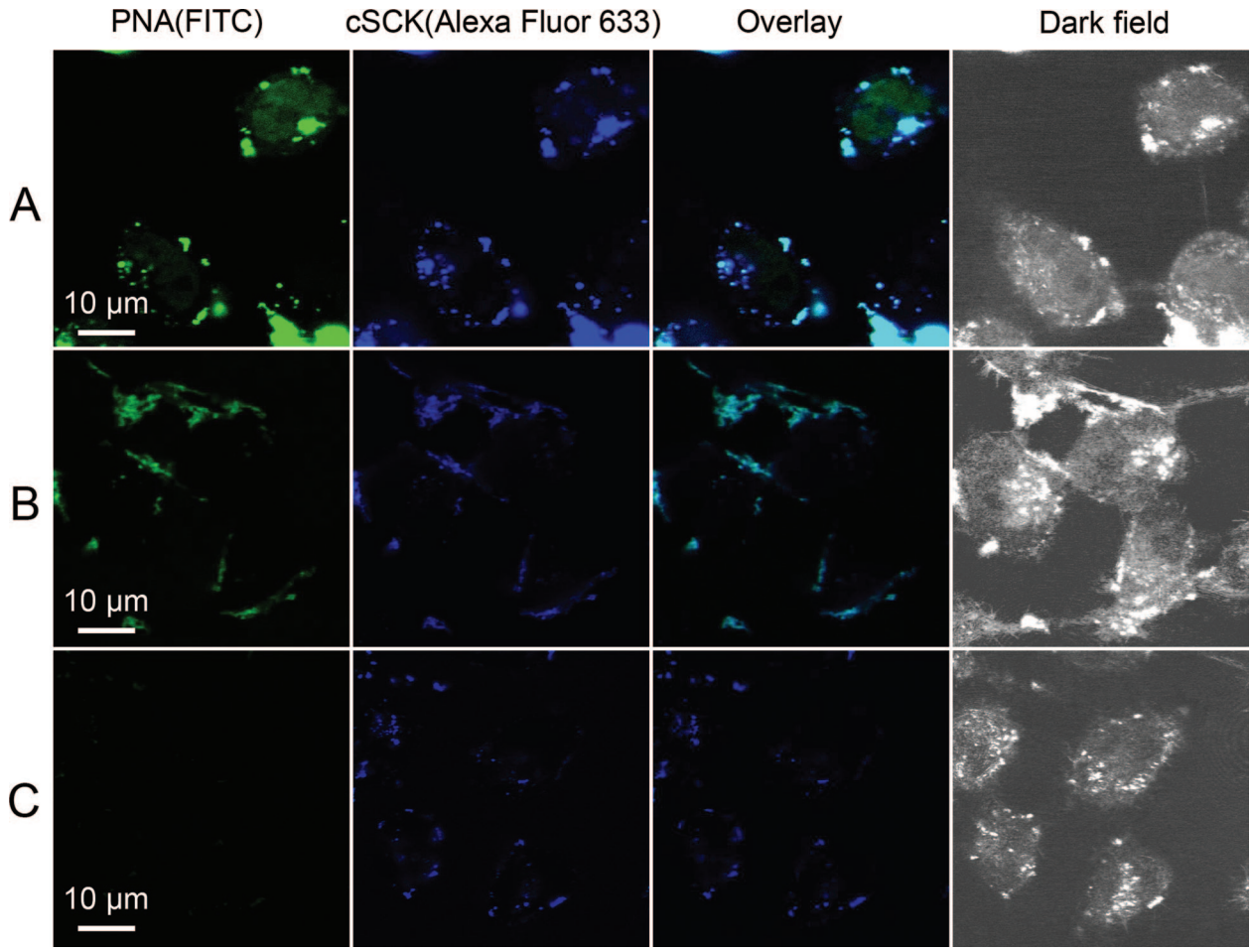

Figure 8. Cell localization of cSCK-SS-PNA and products. pLuc705 HeLa cells were incubated with a dual fluorescently labeled cSCK(Alexa Fluor 633)-SS-PNA(FITC)$_2$, having Alexa Fluor 633 (excitation 633 nm, emission 650 nm) on the cSCK and FITC (excitation 488 nm, emission 510 nm) on the PNA. Row A: 24 h incubation. Row B: 1 h incubation. Row C: 1 h incubation with DTT-pretreated nanoparticles.

The inability of the cSCKs to efficiently escape the endosome would explain the lower activity of the noncleavable cSCK-PNA. Given that the precleaved cSCK also remains trapped in the endosomal compartments, it is likely that transfection of PNA·ODN by cSCK also proceeds by a similar mechanism in which either the PNA·ODN or the PNA alone escapes from the endosome (Figure 1A).

The ability of the cSCK to promote endosomal escape of the PNA could be ascribed to a "proton sponge" effect,[28] in which the remaining basic amino groups on the cSCK react with protons produced during endosomal acidification. As a result of this buffering reaction, the cSCK further enhances the influx of protons, chloride counterions, and water leading to endosomal destabilization and permeabilization by the increased osmotic pressure within the endosome. This process causes the cSCK-SS-PNA$_2$ to be either released into or exposed to the cytoplasm, whereupon the disulfide linkage is cleaved, allowing translocation of PNA to the nucleus. The proton sponge effect has also been recently used to enhance cytosolic delivery of core−shell nanoparticles bearing otherwise impermeable molecules[29] and quantum dots.[30,31]

Conclusions

We have demonstrated that cationic shell-cross-linked knedel-like nanoparticles are highly efficient agents for the delivery of bioactive PNAs into HeLa cells by electrostatic complexation with PNA·ODN hybrids or by conjugation of

(28) Boussif, O.; Lezoualc'h, F.; Zanta, M. A.; Mergny, M. D.; Scherman, D.; Demeneix, B.; Behr, J. P. A versatile vector for gene and oligonucleotide transfer into cells in culture and *in vivo*: polyethylenimine. *Proc. Natl. Acad. Sci. U.S.A.* **1995**, *92* (16), 7297–301.

(29) Hu, Y.; Litwin, T.; Nagaraja, A. R.; Kwong, B.; Katz, J.; Watson, N.; Irvine, D. J. Cytosolic Delivery of Membrane-Impermeable Molecules in Dendritic Cells Using pH-Responsive Core-Shell Nanoparticles. *Nano Lett.* **2007**, *7* (10), 3056–3064.

(30) Duan, H.; Nie, S. Cell-Penetrating Quantum Dots Based on Multivalent and Endosome-Disrupting Surface Coatings. *J. Am. Chem. Soc.* **2007**, *129* (11), 3333–3338.

(31) Yezhelyev, M. V.; Qi, L.; O'Regan, R. M.; Nie, S.; Gao, X. Proton-sponge coated quantum dots for siRNA delivery and intracellular imaging. *J. Am. Chem. Soc.* **2008**, *130* (28), 9006–12.

the PNA *via* a bioreductively cleavable linker. The cSCK at 20 μg/mL results in three times more bioactivity and 2-fold less toxicity than Lipofectamine 2000 at 10 μg/mL when delivering 1 μM PNA·ODN into HeLa cells, and results in a much higher splicing correction efficiency (94% vs 64%). The bioreductively cleavable cSCK-SS-PNA_2 conjugates are similarly effective for HeLa cells at 1 μM PNA, showing only slightly higher cytotoxicity and slightly lower splicing efficiency (85%), but are orders of magnitude better than Arg_9-mediated delivery. The cSCK-SS-PNA system may be very useful for *in vivo* applications, where it would be important to minimize dissociation of the PNA from the cSCK prior to reaching the target cell. Initial mechanistic studies indicate that the cSCK is able to facilitate not only endocytosis but also endosome disruption, thereby facilitating release of the PNA into the cytoplasm from where it can translocate into the nucleus, while the cSCK remains trapped in the endosomal/lysosomal compartments. This type of delivery mechanism may also be quite attractive for *in vivo* purposes if the cSCK can be later exocytosed and excreted, thereby preventing it from accumulating within the cytoplasm of cells. If not, acid- or biodegradable nanoparticles under development could be used. For *in vivo* experiments, we will incorporate DOTA into the polymer side chains to bind ^{64}Cu for PET imaging of cSCK biodistribution and pharmacokinetics. Based on prior experience with SCKs,[32] we also expect that PEG chains will also have to be attached to minimize detection by the RES system and enhance the bioavailability of the cSCKs. The bioactivity of the PNAs could then be assessed through the use of the EGFP-654 transgenic mouse that utilizes EGFP as a reporter for splicing correction.[33] In this way we will be able to determine the extent to which the bioactivity correlates with the bioavailability of the cSCK for different tissues.

Acknowledgment. This work is supported by the National Heart Lung and Blood Institute of the National Institutes of Health as a Program of Excellence in Nanotechnology (NHLBI-PEN HL080729) and by grants to the Washington University NIH Mass Spectrometry Resource (Grant No. P41 RR000954) and Washington University NMR facility (Grant No. RR1571501). We thank Bereket Oquare for the 18-mer PNA, and Zhenghui Wang for obtaining the MALDI data on the PNAs. We also thank G. Michael Veith of the Washington University Department of Biology Microscopy Facility for providing technical support with TEM and fluorescence confocal microscopy, Cindy Fogal of Dr. Kranz's group for help with the luminometer, and Dr. R. Kole (University of North Carolina, Chapel Hill, NC) for the pLuc705 HeLa cell line.

MP800199W

(32) Sun, G.; Hagooly, A.; Xu, J.; Nystrom, A. M.; Li, Z.; Rossin, R.; Moore, D. A.; Wooley, K. L.; Welch, M. J. Facile, efficient approach to accomplish tunable chemistries and variable biodistributions for shell cross-linked nanoparticles. *Biomacromolecules* **2008**, *9* (7), 1997–2006.

(33) Sazani, P.; Gemignani, F.; Kang, S. H.; Maier, M. A.; Manoharan, M.; Persmark, M.; Bortner, D.; Kole, R. Systemically delivered antisense oligomers upregulate gene expression in mouse tissues. *Nat. Biotechnol.* **2002**, *20* (12), 1228–33.